

## 9

---

# Statistical Thermodynamics Through Computer Simulation to Characterize Phospholipid Interactions in Membranes

Mihaly Mezei and Pál Jedlovszky

## Summary

This chapter describes the major issues that are involved in the statistical thermodynamics of phospholipid membranes at the atomic level. The ingredients going into models of lipid bilayers are summarized: force fields, representation of long-range interactions, and boundary conditions. Next, the choice of thermodynamic ensembles, and the two main options for the generation of a representative sample of configurations: molecular dynamics and Monte Carlo are discussed. The final issue that is dealt with describes the various ways the generated ensembles can be analyzed.

**Key Words:** Ewald sum; force field; free-energy profile; molecular dynamics; Monte Carlo; Voronoi tessellation.

## 1. Introduction

Statistical thermodynamic description of a system recognizes the fact that the behavior exhibited by the system cannot be explained by a single state. Instead, the system's behavior is the result of its sampling an ensemble of states. The fundamental result of statistical thermodynamics is the characterization of such ensembles in terms of the Boltzmann distribution. Thermodynamic description of a system can use different sets of independent variables. Once the independent variables are set, other variables are determined by various thermodynamic relations (e.g., the equation of state). Each choice defines a different set of such relationships. Corresponding to each choice of independent variables there is a statistical thermodynamic ensemble, with their respective formalism. Whereas in the infinite system size limit, the results are the same irrespective of the ensemble chosen, for finite sizes they can give answers that differ by an amount that is proportional to  $1/N$ , with  $N$  being the number of particles in the system. Because the formalism is different for each ensemble, the choice is usually governed by computational convenience.

Although analytical theories exist for the characterization of ensembles of simple systems, systems of the complexity of lipid membranes are not amenable to such treatment without extreme simplification. However, such complex systems are amenable to be modeled in full atomic detail using computer simulations. This section presents the various steps involved in characterizing a phospholipid membrane using computer simulation.

## 2. Construction of the System

The construction of a model for a phospholipid membrane involves several choices, each involving some trade-off. The first choice is the representation of intermolecular energies

From: *Methods in Molecular Biology*, vol. 400: *Methods in Membrane Lipids*  
Edited by: A. M. Dopico © Humana Press Inc., Totowa, NJ

and/or forces. Although it would be desirable to use quantum-mechanical techniques, they are still prohibitively expensive. The currently favored choice is the use of molecular mechanical force fields treating nonbonded interactions in a pair-wise additive manner and describing the intramolecular interactions with bond stretching and bending as well as torsional terms, although there exist force fields that also include cooperative terms, usually represented as polarization energy. Statistical treatment in general assumes a large enough sample that the average behavior of the sample is representative of the full-size system. The larger the number of molecules in the model, the better the representation, yet the calculation is more expensive. The accuracy of a model with limited number of molecules is increased significantly by the use of periodic boundary conditions: a basic cell containing the system is surrounded by periodic replicas in all three dimensions. This device eliminates surface effects at the expense of introducing artifactual periodicity into the model.

## 2.1. Force Field

### 2.1.1. All-Atom Representation

Molecular mechanical force fields express the energy of the system  $E(X^N)$  as a sum of several terms and—when needed—calculate the force acting on each atom as the gradient of this energy:

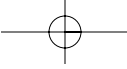
$$E(X^N) = E_{\text{NB}} + E_{14} + E_{\text{BOND}} + E_{\text{ANG}} + E_{\text{TOR}} \quad (1)$$

where  $E_{\text{NB}}$  is the nonbonded energy, summed over all pairs of atoms  $X_i$  and  $X_j$ , separated by the distance  $r_{ij}$ , that are on different molecules or in the same molecule but separated by more than three bonds,  $E_{14}$  is the nonbonded energy summed over all pairs of atoms separated by exactly three bonds, and  $E_{\text{BOND}}$ ,  $E_{\text{ANG}}$ , and  $E_{\text{TOR}}$  are the intramolecular energies summed over all bonds, bond angles, and torsions, respectively. The nonbonded term is usually given in the form

$$E_{\text{NB}}(X_i, X_j) = 4\epsilon \left[ \left( \frac{\sigma}{r_{ij}} \right)^{12} - \left( \frac{\sigma}{r_{ij}} \right)^6 \right] + \frac{q_i q_j}{r_{ij}} \quad (2)$$

where  $\epsilon_{ij}$  and  $\sigma_{ij}$  are the so-called Lennard-Jones parameters, representing the depth of the attraction owing to dispersion forces and the extent of exchange repulsion, respectively;  $q_i$  and  $q_j$  are the partial charges assigned to atoms  $i$  and  $j$  to represent the electrostatic interaction between them. Although some force fields assign  $\epsilon_{ij}$  and  $\sigma_{ij}$  values for different pairs of atom types, most assign values for each atom type and obtain  $\epsilon_{ij}$  and  $\sigma_{ij}$  as a combination of the two. The combination rules either involve calculating the geometric mean of both (e.g., in the OPLS force field [1]) or the so-called Lorentz-Berthelot rule: arithmetic mean for  $\sigma_{ij}$  and geometric mean for  $\epsilon_{ij}$  (e.g., in force fields CHARMM [2] and AMBER [3]). Partial charges are either obtained from empirical rules (see ref. 4) or from *ab-initio* calculations, using a fitting procedure that finds partial charges by ensuring the best reproduction of the electric field around a molecule. In general, the Lennard-Jones parameters are established independently of the molecule the atom is in; partial charges are assigned for each molecule.

It is important to keep in mind two facts that may eventually result in fundamental reparametrization of nonbonded interactions. First, this form, although well established (even entrenched), owes its existence to the necessity of saving computational time at the expense



of introducing too steep repulsion. Second, whereas the three terms appear to neatly represent the physics of three different types of interactions (exchange repulsion, dispersion, and electrostatics), when performing a least-squares fit to actual data the matrix obtained is usually nearly singular, indicating that the functions proportional to  $r^{-12}$ ,  $r^{-6}$ , and  $r^{-1}$  are nearly linearly dependent. Besides the practical problem of having to deal with nearly singular matrices this means that the coefficients derived will contain contributions from different types of interactions. As a result, the transferability of the parameters suffers.  $E_{14}$  is represented with the same functional form as  $E_{\text{NB}}$ , but either with a different set of nonbonded parameters (e.g., in CHARMM) or applying an overall correction factor to both the Lennard-Jones and the electrostatics part (e.g., in AMBER).

$E_{\text{BOND}}$  and  $E_{\text{ANG}}$  are generally represented with harmonic terms:

$$E_{\text{BOND}} = k_{ij}^b (r_{ij} - r_{ij}^0)^2, \quad (3)$$

and

$$E_{\text{ANG}} = k_{ijk}^a (\alpha_{ijk} - \alpha_{ijk}^0)^2 \quad (4)$$

or

$$E_{\text{ANG}} = k_{ik}^{\text{UB}} (r_{ik} - r_{ik}^0)^2, \quad (5)$$

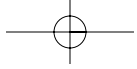
where  $i$  and  $j$  are the atoms forming the bond of length  $r_{ij}$ ,  $i$ ,  $j$ , and  $k$  are the atoms forming the bond angle  $\alpha_{ijk}$ , the superscript 0 refers to the equilibrium value, and the parameters  $k^a$ ,  $k^b$ , and  $k^{\text{UB}}$  are the respective harmonic strengths. The second form of  $E_{\text{ANG}}$  is usually referred to as the Urey–Bradley term.  $E_{\text{TOR}}$  represents in general two types of terms. The contribution of the conformational state of a bond to the energy of the molecule is usually expressed as a trigonometric function of the torsion angle  $\delta$ :

$$E_{\text{TOR}} = k_{ijkl} [1 + \cos(n_{ijkl} \delta_{ijkl} + \delta_{ijkl}^0)], \quad (6)$$

where the parameter  $k_{ijkl}$  represents the strength of the interaction, and the parameters  $n_{ijkl}$  and  $\delta_{ijkl}^0$  depend on the type of the bond. The other type is called improper torsion and is used to enforce either the chirality of an atom or to keep a bond in a plane (e.g., in the case of an aromatic ring). For an atom  $k$  with bonded neighbors  $i$ ,  $j$ , and  $l$ , the improper torsion is a harmonic function of the angle between the planes formed by atoms  $i$ ,  $j$ , and  $k$  and by atoms  $j$ ,  $k$ , and  $l$ . It cannot be emphasized enough that the various terms of each extensively used force field have evolved as a whole, and mixing terms from various sources is likely to lead to inferior results.

### 2.1.2. Simplified Lipid Representation

There have been efforts to reduce the computational expense by introducing simplifications into the all-atom representation in such a way that the essence of the interactions is conserved. Foremost among such simplification is the simplified treatment of hydrogens. Both CHARMM and AMBER have parameter sets wherein the apolar hydrogens have been mapped onto the carbon atom they are bonded to. In this treatment, there will be different carbon atom types depending on how many hydrogens are mapped. An intermediate solution



was presented by the GROMACS force field (5) that introduced the concept of frozen groups: hydrogens do appear explicitly but their movement is not independent of the heavy atom they are bonded to.

As even without explicit hydrogens the time-scale available for simulating lipid bilayers is generally inadequate to study rare events, such as the exchange of lipids between bilayers (also called “flip–flop transitions”), further simplifications have been introduced (6–9). These models concatenate the headgroup into a few hydrophilic centers and replace the hydrophobic tails with a few centers connected with a harmonic spring. Such models are able to reproduce even the spontaneous formation of the membrane bilayer within reasonable computer time (7).

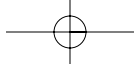
## 2.2. Periodic Boundary Conditions

The most important property required of a simulation cell used under the traditional periodic boundary conditions is that it can be used to pack the three-dimensional space by appropriately translated copies of itself without leaving void space. The conceptually simplest of such shape is the cube. However, as the periodic system is used only to avoid having to introduce a surface, the effect of periodicity should be minimized. In simulating general solutions, this calls for a shape that has the largest inscribed sphere for a given volume and led to the introduction of rhombic dodecahedron and truncated octahedron. In modeling lipid bilayers the distance between layer images should be kept as large as possible because the concerted effect of a bilayer is much stronger than the interaction between individual lipids in the same layer. This led to the use of prism shape cells for lipid bilayers wherein the axis of the prism is along the bilayer normal. Consistent with the use of prism, one can still use a cross-section that has the largest inscribed circle for a given area, leading to the choice of hexagonal prism (10).

Simulations of lipid bilayers can take advantage of periodic systems wherein the replicas of the simulation cell filling the space seamlessly are generated by translation and rotation. Dolan et al. (11) have shown that using either  $P2_1$  or  $Pc$  symmetry the neighboring box will contain an image of the *opposite* layer. Under these symmetries the two layers can end up exchanging lipids *without actually flipping over* because a lipid leaving the cell at one side will cause its image to re-enter the simulation cell in the opposite layer. This provides a computationally efficient way to equilibrate the two layers of a membrane (an important task if the two layers have different guests embedded into them). Without using one of these nontraditional periodic boundary conditions, such an equilibration requires either the direct exchange of lipids between the two layers or the separate determination of the requisite number of lipids based on the area/headgroup of the lipids and the guest. The first solution is computationally impractical, whereas the reliability of the second is questionable. Thus, it is somewhat of a surprise that use of these boundary conditions has not been widely adopted for the modeling of lipids with proteins embedded, as witnessed by a recent review on such simulations (12).

## 2.3. Treatment of Long-Range Interactions

In general, the energy of interaction between two atoms decreases with the distance between them. Thus, significant savings in computer time can be achieved by treating interactions between distant atoms separately from interactions between pairs closer to each other. One option is to set them to zero when the distance exceeds some predefined threshold, usually called cutoff. The other option is to use a simplified representation of interactions



between distant pairs. In the context of simulating lipid membranes this takes the form of using a formalism to obtain the interaction with simplified forms of all periodic cells, extending to infinity, realized by a construct called Ewald sum (see **Subheading 2.3.2.**).

### 2.3.1. Cutoffs

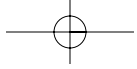
If interactions among all atoms of the system were to be calculated, the computation cost (even assuming pair-wise additive potentials) would be proportional to the *square* of the number of atoms. However, the interactions die off as the distance between them increases, so such a procedure would result in calculating many near-zero quantities. This observation prompted the introduction of cutoffs: a distance threshold beyond which all interaction energies are assumed to be zero. However, this procedure is not without pitfalls. Besides the obvious problem of being “greedy” and choosing too short of a threshold, there are the problems created by the discontinuity at the cutoff distance (causing artifactual heating during molecular dynamics runs) and the neglect of contributions from the small but numerous distant pairs that can add up to a significant amount even when the choice of threshold was not “greedy.” The discontinuity, only affecting adversely molecular dynamics simulations, can be eliminated by the introduction of a so-called switching function that continuously changes the function to be cutoff at zero over a finite interval. The cumulative contribution of pairs beyond the distance  $R_C$  whose interaction is proportional to  $1/r^k$  has the general form of

$$\int_{R_C}^{\infty} \frac{C}{r^k} r^2 dr = \frac{C}{k-3} \left[ \infty^{-k+3} - R_C^{-k+3} \right] \quad (7)$$

For large enough  $R_C$  this provides significant contribution only if the interactions die off slower than  $1/r^4$ . For  $k = 3$  (as is the case for dipole–dipole interactions) the integral will depend on the way the triple integration is carried out, i.e., on the shape of the system as it is extended to infinity. For  $k < 3$  (as is the case of charge–charge and charge–dipole interactions) the integral diverges for sure. To avoid such problem it has been recognized early on (**13**) that, whenever possible, atoms should be grouped into neutral clusters and the cutoff between any two atoms should be based on the distance between the cluster centers.

### 2.3.2. Ewald Sum

In general the total dipole moment of a simulation cell is nonzero. Thus, the electrostatic interactions between a simulation cell and its periodic replicas can add up to a significant amount. However, the summation of these terms is nontrivial: the resulting infinite series is only conditionally convergent. As a consequence, the final sum depends on the order of summation, just as the integral of the distant dipolar contributions depend on the shape of the system being integrated to infinity. Ewald (**14**) introduced a technique that calculates the dipolar sum as two absolute convergent series, one of them in the reciprocal space. The relation between the Ewald sum and the summation order has been analyzed by Campbell (**15**). Use of the Ewald sum has been facilitated by the introduction of the particle-mesh technique (**16**) that significantly reduced its computational complexity. However, note that its use corresponds to a system on infinite stack of bilayers (separated by water layers) instead of a single bilayer. To avoid this artifact, the Ewald technique has been extended to systems that are periodic in only two of the three spatial dimensions (**17**).



### 3. Generation of Boltzmann Sample of Configurations

There are three different decisions that have to be made when establishing the procedure for generating a Boltzmann-weighted ensemble: (1) the choice of thermodynamic ensemble, (2) the method of sampling in the ensemble chosen, and (3) as all methods of sampling obtain successive configurations from the previous one, the generation of the initial configuration.

#### 3.1. Thermodynamic Ensembles

The thermodynamic ensembles most frequently used include the canonical ( $N, V, T$ ), microcanonical ( $N, V, E$ ), isothermal-isobaric ( $N, p, T$ ), and grand-canonical ( $\mu, V, T$ ) ensembles. For modeling membrane systems sometimes the surface tension is also included as an additional variable, leading to simulations in the ensemble ( $N, p, \gamma, T$ ) (18,19). The choice of the ensemble is made based on the importance of which thermodynamic property has to be guaranteed to give the right (i.e., experimental) value and the sampling advantage a particular ensemble offers. By setting  $V$  and  $N$  constant, the density (and for lipid bilayers, the area/headgroup) can be set to the desired value but the pressure will be obtained from the simulation, and because of the approximate nature of the force field, it cannot be guaranteed to turn out to be 1 atm. However, for heterogeneous systems the density is a complex function of the components, and assuming the incorrect value may lead to the appearance of large voids (bubbles) in the system.

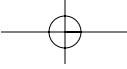
Classical molecular dynamics corresponds to sampling in the microcanonical ensemble, but the technique has been generalized to other ensembles by including an additional fictitious degree of freedom. The choice of the ensemble also affects the sampling efficiency. Using constant  $p$  (and  $\gamma$ ) requires periodic change in the volume (and in the cross-section of the cell), helping the system to cross barriers. Using constant  $\mu$  requires the change in the number of particles (i.e., insertions and deletions) and this helps equilibration between different pockets or semipockets of the system in general and speeds up the penetration of the solvent by an order of magnitude (10). Whereas successful insertions into condensed phase systems are generally rare, the cavity-biased technique made efficient use of the ( $\mu, V, T$ ) ensemble feasible (20,21).

#### 3.2. Method of Sampling

Currently, two major classes of methods are used for sampling configurations of condensed phases: molecular dynamics and Monte Carlo (MC). Molecular dynamics takes advantage of the fact that systems following Newton's law of motion will sample a Boltzmann-distributed ensemble, whereas MC methods use the mathematical construct called Markov chain that can also generate a Boltzmann-distributed ensemble. From a mathematical point of view, the MC approach solves a problem with weaker restrictions than molecular dynamics because satisfying Newton's law of motion is a sufficient but not necessary condition for the generated set to follow a Boltzmann distribution. However, current practice favors molecular dynamics as it was found to work well and the few realizations of MC attempted so far have not proven to be superior to it. However, it is our belief that the potential of the MC approach has not been fully exploited yet (22). Note also that simulations can combine the two techniques to exploit the respective advantages of each (23–25).

##### 3.2.1. Molecular Dynamics

The large number of degrees of freedom in a system of solvated lipid bilayers implies that Newton's law of motion has to be solved by numerical quadratures. There are several of such



quadratures developed (see ref. 26), but each is limited in the time step they can make in order to maintain conservation of energy. Some increase in the time step is possible if the highest frequency motions (i.e., the vibrations involving hydrogen atoms) are frozen. This is usually achieved by applying a constraint on the bond lengths (usually implemented by the SHAKE method [27]) involving hydrogens, allowing the increase of the time step from the customary 1–2 fs.

### 3.2.2. Monte Carlo

The MC technique used for simulation of atomic and molecular assemblies, usually referred to as the Metropolis method (28), is based on the construction of a Markov chain whose limiting distribution  $\pi$  is the Boltzmann distribution in the ensemble under consideration. This requires the construction of a transition matrix  $P$  such that  $\pi = P\pi$ .  $P$  is constructed with the help of another matrix  $Q$  whose elements  $q_{ij}$  form a transition matrix of an irreducible Markov chain on the same states. The  $q_{ij}$  matrix elements are usually referred to as the *a priori* transition probabilities. The simulation proceeds from state  $i$  by selecting a candidate state  $j$  with probability  $q_{ij}$  that is accepted with probability (26).

$$P_{\text{acc}} = \min\left(1, \frac{\pi_j q_{ij}}{\pi_i q_{ji}}\right) \quad (8)$$

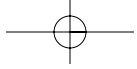
The original Metropolis method uses the particular choice of  $q_{ij} = q_{ji}$ . In general, the shift from state  $i$  to state  $j$  changes a small part of the system, to avoid having too small ( $\pi_j / \pi_i$ ) in the above equation. The aim of the sampling technique design is to select the largest possible change in the system that is still likely to be accepted. This is achieved by the judicious choice of coordinates for the change and for the magnitude and direction of change. For the sampling of polymer conformations, such as lipids, this usually means the use of torsional coordinates. The choice of sampling techniques is only limited by the practitioners' imagination. Here three such techniques that have been applied to lipid simulations or are considered having strong potentials are briefly described.

#### 3.2.2.1. CONFIGURATIONAL BIAS MC

Configurational bias MC generates new elements of the Markov chain by growing (possibly only part of) a polymer chain unit by unit, adding each by considering the other atoms in the vicinity to minimize steric overlap; the bias introduced by these choices can be controlled and corrected for (29,30). The most attractive feature of this technique is the significantly reduced correlation between successive accepted members of the Markov chain. However, as the system becomes denser, the probability of acceptance becomes progressively smaller.

#### 3.2.2.2. EXTENSION-BIAS MC

Extension biasing is based on the observation that the maximum atomic displacement resulting from a given torsion angle change depends on the shape of the part of a molecule that is affected by the change in that torsion angle; it scales the torsion angle stepsize parameter with the inverse square root of the largest distance from the torsion axis (10). So far it was applied to torsions that move the full length of the polymer chain, but it is equally applicable to local moves affecting only a polymer segment (31,32) (although it has not been done yet).



### 3.2.2.3. SCALED COLLECTIVE VARIABLES

Sampling in terms of the so-called scaled collective variables (33) is a well-established technique that finds a special linear combination of natural variables (e.g., torsion angles) that result in significantly better sampling. The coefficients are obtained from the eigenvectors and eigenvalues of the Hessian of the system, with a significant additional computational expense being involved. Although (to the authors knowledge) it has not been applied to lipid systems, a novel and efficient implementation could calculate the Hessians separately for each lipid instead of calculating a single Hessian for all of the lipids, as this reduces the computational complexity of calculating Hessians by a full order of magnitude.

## 3.3. *Initial Configuration*

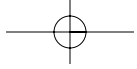
With lipid simulations becoming more and more widespread, reasonably well-equilibrated initial configurations can be obtained from earlier simulations of the same or similar systems. Lacking such “crutch,” condensed phase simulations start either from a randomly generated configuration or from a crystalline state (corresponding to a start at infinite or zero absolute temperature, respectively). For simulations of a lipid bilayer these choices are likely to be both extremely inefficient because the time-scales of both lateral diffusion and orientational relaxation in a bilayer indicate that providing a well-equilibrated system at ambient or physiological temperatures would require very long simulations. In spite of this dire prognosis such calculations have been performed successfully (34). A well-established strategy to build a new bilayer (35) is random selection of phospholipids from a preequilibrated and prehydrated library of DPPC generated by MC simulations in the presence of a mean field (36,37).

## 4. Analysis of the Generated Ensemble

### 4.1. *Density Profiles*

In characterizing the average structure of the membrane at different regions along its normal axis probably the most important tool is the density profile of various atoms or atomic groups. The calculation of density profiles is a rather straightforward task: the average occurrence of the atoms of interest per configuration has to be counted in different lateral slices of the membrane and divided by the volume of the slice. To obtain better statistics it is generally advised to average the obtained profiles over the two layers of the membrane. Conversely, the comparison of the density profiles in the two separate layers can provide information on the sampling efficiency of the equilibrium structure of the membrane layers.

To get an overall view about the distribution of the atoms across the membrane the mass and electron density profiles of the system are of particular importance. The relevance of the calculation of electron density profile in simulations is stemmed from the fact that it can also be measured in X-ray diffraction experiments, and hence it is one of the important properties of the system through which the quality of the simulation can directly be tested against experimental data. The general shape of the mass and electron density profiles in phospholipid membranes shows that the highest and lowest density part of the membrane is the region of the headgroups and the middle region of the chain terminal  $\text{CH}_3$  groups, respectively. The distance of the density peaks corresponding to the two headgroup regions is a simple measure of the membrane thickness. Furthermore, the absence or presence of a thin but deep minimum



in the middle of membranes of more than one component can provide information on whether all the components can extend to the middle of the bilayer or not (38,39).

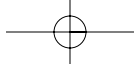
Besides the overall density profiles of the system, the density profile of various atomic groups can also provide valuable information on the organization of the membrane structure along its normal axis. Thus, the density profile of the water molecules shows how deeply water can penetrate into the bilayer. The evolution of this profile during the simulation is a rather sensitive measure of the equilibration of the system (10). This profile can also easily be converted to the free energy profile of water up to the position beyond which the obtained water density reaches zero. Although any meaningful analysis of such density profiles usually requires their determination across the entire membrane, the distance range within which the rather computationally demanding calculation of the water free energy profile has to be performed can substantially be reduced in this way (40).

The density profiles of various atomic groups can also be considered when the system investigated has to be divided into separate regions. Such a partitioning of the membrane can be useful in the analysis of various structural or dynamical features that show considerable variation along the membrane normal axis owing to the large inhomogeneity of the system. In this way, the properties of interest can be separately analyzed in the separate membrane regions. The usual partitioning of the membrane divides it to regions dominated by the hydrocarbon chains, the headgroups, and the hydrating water molecules, respectively. However, based on the density profiles of various atomic groups, more sophisticated yet physically still meaningful dividing schemes can also be derived (40,41).

The comparison of the density distribution of different atoms or atomic groups along the membrane normal axis can also give some indication on the average alignment of various parts of the lipid molecules. Thus, for instance, the comparison of the density profiles of the P and N atoms (18,24,38–40,42), or the negatively charged phosphate and positively charged choline groups (43–47) in pure membranes of phosphatidylcholine lipids has revealed that, although the N atom or choline group density peak is somewhat farther from the middle of the bilayer than that of the P atoms or phosphate groups, the two density peaks largely overlap with each other. This observation indicates that the dipole vector of the lipid headgroups (roughly pointing from the P to the N atom) is, on average, directed more likely toward the aqueous phase than toward the membrane interior; however, this preference is rather weak. This conclusion, drawn solely from the behavior of density profiles has also been confirmed by detailed analyses of the headgroup structure (18,38,39,48–51).

#### 4.2. Order Parameter

In the liquid crystalline ( $L_\alpha$ ) phase of the membrane the conformation of the hydrocarbon tails of the lipid molecules is disordered. This conformational disorder can be characterized by various different quantities, such as the average tilt angle of each of the C–C bonds along the hydrocarbon tails (39,52) or the ratio of the appearance of the *trans* and *gauche* alignments of the dihedral angles around these bonds (42,53–55). However, the vast majority of the studies calculate the profile of the  $\text{CH}_2$  group order parameter along the lipid tails for characterizing their conformational and orientational order. The importance of the determination of the order parameter profile in the simulation is that it can also be measured by nuclear magnetic resonance spectroscopy, and thus, it is another quantity through which the simulation results can be compared with experimental data.



The order parameter tensor of a  $\text{CH}_2$  group is defined as

$$S_{ij} = \frac{\langle 3 \cos \gamma_i \cos \gamma_j - \delta_{ij} \rangle}{2}, \quad (9)$$

where indices  $i$  and  $j$  run through the  $x$ ,  $y$ , and  $z$  axes of the local Cartesian frame fixed to the  $\text{CH}_2$  group,  $\gamma$  is the angle formed by the corresponding axis of this frame with the membrane normal,  $\delta_{ij}$  is the Kronecker  $\delta$ , and  $\langle \dots \rangle$  denotes ensemble averaging. The local frame is defined in such a way that its  $x$ -axis connects the two H atoms, the  $y$ -axis is the main symmetry axis of the  $\text{CH}_2$  group, whereas the  $z$ -axis is perpendicular to the plane of the three atoms. In the case of using a force field of simplified lipid representation (i.e., when the entire  $\text{CH}_2$  group is treated as a united atom) this frame has to be defined without knowing the orientation and geometry of the  $\text{CH}_2$  group. However, a definition equivalent with the aforementioned one can still be given in this case. Thus, the  $z$ -axis connects the C atoms located before and after the  $\text{CH}_2$  group of interest along the hydrocarbon chain, the  $y$ -axis is perpendicular to  $z$  and lays also in the plane containing the  $\text{CH}_2$  group of interest and its two neighboring C atoms, whereas the  $x$ -axis is perpendicular to both  $y$  and  $z$  (56).

The deuterium order parameter  $S_{CD}$  that is measurable by nuclear magnetic resonance spectroscopy is related to the elements of the order parameter tensor through the relation

$$S_{CD} = \frac{2S_{xx} + S_{yy}}{3} \quad (10)$$

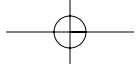
Because of the symmetry of the  $\text{CH}_2$  group the  $S_{xy}$  and  $S_{xz}$  elements of the order parameter tensor are zero. Furthermore, isotropic rotation around the  $z$ -axis leads to the relations of  $S_{yz} = 0$  and  $S_{zz} = -2S_{xx} = -2S_{yy}$  (57) (the  $S_{zz}$  parameter is often referred to as  $S_{\text{chain}}$  as well.). In this case, the  $S_{CD}$  order parameter of a given  $\text{CH}_2$  group can simply be calculated as

$$S_{CD} = \left\langle \frac{3}{2} \cos^2 \alpha - \frac{1}{2} \right\rangle, \quad (11)$$

where  $\alpha$  is the angle formed by the C–H bond with the membrane normal. Conversely, a noticeable deviation of the obtained  $S_{zz}$  values from  $-2S_{xx}$  or  $-2S_{yy}$  indicates the existence of rotational anisotropy along the molecular axis joining two C atoms that are separated by two C–C bonds (56).

#### 4.3. Structure of the Headgroup Region

The structure of the dense headgroup region of the membranes, consisting of the polar part of the constituting lipid molecules, the waters penetrated deepest into the bilayer, and also fractions of the hydrocarbon chains is of key importance in determining the properties of the membrane. The headgroup structure is resulted from the delicate interplay between the lipid–lipid and lipid–water interactions. The overall organization of the polar lipid headgroups and waters hydrating them can be characterized by the electrostatic potential between the aqueous phase and the membrane interior, a quantity that can again be compared with experimental data, and its contributions because of the lipid and water molecules. The detailed description of the headgroup region structure includes the analysis of the lipid headgroups as well as the structure of the interfacial water.



#### 4.3.1. Electrostatic Potential

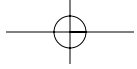
The electrostatic potential difference between the aqueous phase and the interior of the membranes built up by neutral phospholipid molecules results from the microscopic separation of the center of the positive and negative charges owing to the orientational preferences of the lipid headgroups and water molecules. This electrostatic potential difference, often referred to as the dipole potential  $\Phi$ , can be calculated using the Poisson equation at the distance  $Z$  from the middle of the bilayer along its normal axis as the double integral of the charge density profile  $\rho_Q(Z)$ :

$$\Phi(Z) = -\frac{1}{\epsilon_0} \int_0^Z dZ' \int_0^{Z'} \rho_Q(Z'') dZ'', \quad (12)$$

where  $\epsilon_0$  is the vacuum permittivity. It is not surprising that the contribution of the lipid and water molecules to this potential is of opposite sign: the orientation of the water dipole vectors is driven by the charge distribution of the lipid headgroups along the membrane normal axis. Owing to the fact that the positively charged group of the neutral phospholipid molecules is always located at the end of the headgroup chain, and hence they are, on average, farther from the bilayer center than the negatively charged phosphate group that is attached directly to the glycerol backbone, the lipid contribution to the electrostatic potential of the aqueous phase with respect to the membrane interior is positive. However, this positive potential is usually overcompensated by the negative potential contribution because of the preferential orientation of the water molecules, resulting in a net negative electrostatic potential value in the aqueous phase (24,45,50,58,59), which is in agreement with existing experimental data (60).

#### 4.3.2. Lipid Headgroup Structure

Perhaps the most important property characterizing the structure of the lipid headgroups is the distribution of its tilt angle relative to the membrane normal (the orientation of the phosphorylcholine headgroup is often described by the vector pointing from its P to N atom, called the PN vector, *see refs. 18,38,39,48–51*). However, a detailed analysis of the headgroup structure requires a thorough investigation of the interactions acting between the headgroups as well. Because phospholipid molecules lack hydrogen bond donor H atoms, the most prevalent interactions acting between neighboring headgroups are charge pairing (49) and water bridging (i.e., when the two lipid headgroups are forming hydrogen bonds with the same, bridging water molecule) (61). In addition, in the case of mixed membranes containing also H-donor molecules (e.g., cholesterol) hydrogen bonding can also occur between these molecules and phospholipids (62). The presence and relative importance of these interactions as well as their details (e.g., participating atoms, equilibrium distance) can be analyzed in detail using the partial pair correlation function of appropriately chosen atom pairs (40,42,47–49,61–66). Because the lateral packing of the molecules is mainly determined by the interactions acting between the headgroups, the detailed investigation of the local lateral structure (e.g., by Voronoi analysis) can also shed some light to the nature of the headgroup–headgroup interactions (65,67,68). Furthermore, the relative arrangement of the neighboring headgroups can be described by the distribution of the angle formed by the vectors describing their orientation (usually the PN vector) (66), whereas their spatial distribution around each other can well be characterized by the distribution of the angle formed by two



neighboring headgroups (represented by the position of an appropriately chosen atom, e.g., P or N) around the central one.

#### 4.3.3. Structure of the Interfacial Water

The change of the orientational order of the interfacial water molecules along the membrane normal axis can be characterized by the profiles (i.e., the average values obtained in different lateral membrane slices) of appropriately chosen orientational parameters (51,58). Based on the behavior of these profiles the headgroup region can be divided into separate layers in which the full distribution of these orientational parameters can then be meaningfully analyzed (58). In phospholipid membranes, as in other polar interfaces the most important orientational parameter in this respect is clearly the angle formed by the water dipole vector with the membrane normal axis. However, the description of the alignment of entire water molecules relative to the bilayer requires the introduction of other orientational parameters as well. In analyzing the interfacial orientation of water molecules it should be kept in mind that the unambiguous description of the orientational preferences of a rigid molecule relative to an external vector (e.g., the membrane normal) requires the calculation of the bivariate joint distribution of two independent orientational variables (e.g., the angular polar coordinates of the external vector in a local frame fixed to the individual molecules) (69,70).

### 4.4. Analysis of Voids

The properties of the voids in lipid membranes are closely related to the key biological functions of the membranes. Thus, several small molecules of vital physiological importance (e.g., O<sub>2</sub>, CO<sub>2</sub>, NO, and so on) go through the membrane of the cells by passive transport. This diffusion process is obviously related to the properties of the voids in the membrane. Furthermore, some theories explain the phenomenon of anesthesia partly by changes in the void distribution of the membranes owing to the anesthetics that are dissolved in the membrane interior (71). The properties of the voids to be calculated in order to thoroughly characterize the organization of the free volume in the system include the distribution of their size, shape, connectivity, and orientation in the different regions of the membrane. In defining voids, a distinction has to be made between the *empty* free volume (i.e., the entire space that is not covered by the atomic spheres) and the *accessible* free volume (i.e., the free volume pockets that are accessible for a spherical probe of a given size) (72). Obviously, the determination of the accessible free volume requires the introduction of an extra parameter (i.e., the radius of the probe). In the limiting case of the probe radius of zero the accessible and empty free volumes become equivalent. Voids in the membrane can either be detected using a set of test points, or analytically using the Voronoi–Delaunay (VD) method (73).

#### 4.4.1. The Test Point Approach

In this method a large set of test points are generated (either randomly or along a grid) in the system, and the points that are farther from all the atoms of the system than a given limiting distance are marked. The ratio of these marked points and the total number of points generated provide immediately the fraction of the accessible free volume corresponding to the probe radius equal to the limiting distance used in the procedure (45,68,72,74–76). However, the identification of the voids is a rather difficult task, because it has to be done on a system of marked and unmarked discrete points. A computationally efficient way of solving this problem involves union/find type algorithm that results in a tree structure containing

the information on how the marked sites are connected to each other (76). A more serious problem of the test point approach is that it introduces a certain numerical inaccuracy in the results. To keep this numerical inaccuracy sufficiently low, a large number of test points has to be used, which makes the entire analysis computationally rather costly. Furthermore, the computational cost of such calculations increases proportionally with the cube of the system size.

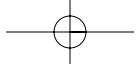
#### 4.4.2. The VD Method

In analyzing voids in systems built up by large molecules, such as lipid membranes, a generalized variant (77) of the original VD method (73) has to be used. In this approach, the system is divided into cells, which are called the Voronoi S-regions. Each of these cells is associated with an atom, and covers the region of space every point of which is closer to the surface of this particular atom than to any other atom of the system. Obviously, these cells fill the space without gaps and overlaps. The faces, edges, and vertices of these cells are the loci of the spatial points that are equally close to the surface of two, three, and four atoms, respectively, and are closer to these atoms than to any other atom of the system. Thus, the vertices of the Voronoi S-regions are the centers of the empty interstitial spheres that can be inscribed between the atoms of the system. These spheres can be regarded as elemental cavities; any complex void present in the system is built up by them. Furthermore, each edge of a Voronoi S-region connecting two of its vertices represents the fairway passing through the narrow bottleneck between the nearest atoms, and can be characterized by the radius of this bottleneck. The set of the Voronoi S-network vertices and edges of the system are forming a network, called the Voronoi S-network that can be used to map the interatomic voids in the system. Thus, each void accessible by a given spherical probe can be represented by a connected cluster of the S-network edges, the bottleneck radius of all of which exceeds the radius of the probe. Knowing the position and radius of the atoms as well as of the elemental interatomic cavities (represented by the S-network vertices) the volume of the void can easily be calculated (77). Although the determination of the Voronoi S-network vertices and edges requires rather sophisticated algorithms, this approach can detect the voids present in the system in an exact yet computationally less demanding way (41,77,78).

### 4.5. Analysis of the Solvation

#### 4.5.1. Solvation of Large Molecules

The ultimate goal of the lipid membrane simulations is to model the complex environment of the membranes of living cells, and thus, help in understanding their biological functions on the molecular level. However, presently available computer capacities only allow the simulation of a few solute molecules, for example, anesthetics (79,80), coenzymes (81), peptides (82), oligonucleotides (83), or a protein molecule (12) in a pure phospholipid membrane, or simulations of two component mixed membranes built up by phospholipid molecules as the main component and other natural amphiphils (e.g., cholesterol, *see refs.* 23,24,38,39,45,54,62,63,65,68,75,76,78). Recently, Pandit et al. (84) have reported computer simulation of a three-component rafted membrane in which a domain of cholesterol and 18:0 sphingomyelin is embedded in the matrix of phospholipid molecules. These studies usually focus on the local (23,65,76,82) as well as overall (24,38,39,45,68,76,78–84) changes induced in the structure of the phospholipid membrane by the solutes, the specific (e.g., hydrogen bonding) interactions between the solute and phospholipid molecules (62,63,65,83), as well as on the preferential position and diffusion of the solute in the membrane (79–81).



#### 4.5.2. Free Energy Profile of Small Molecules and Membrane Permeability

For a class of solvent molecules of biological relevance, i.e., small, neutral molecules of physiological importance (e.g., water, O<sub>2</sub>, CO<sub>2</sub>, NO, and so on), solvation in the membrane can be analyzed in considerably more detail than that of larger solutes. The biological role of these molecules requires their ability of passing through the membrane without the aid of any specific, membrane-bound proteins, and hence the profile of their solvation free energy across the membrane is of great importance. Such calculations (40,74,75,85,86) are usually performed by inserting the solute into a large set of test points in the system. Using the cavity insertion variant of the method (74), when the test particle is only inserted into spherical cavities of the minimum radius of  $R_{\text{cav}}$ , the free energy profile  $A(Z)$  along the membrane normal axis  $Z$  can be computed as

$$A(Z) = -k_{\text{B}}T [\ln \langle \exp(-U_{\text{test}}(Z)) \rangle / k_{\text{B}}T + \ln \langle P_{\text{cav}}(Z) \rangle - 1] - pV/N, \quad (13)$$

where  $k_{\text{B}}$  is the Boltzmann constant,  $N$  is the number of the particles,  $p$ ,  $V$ , and  $T$  are the pressure, volume, and absolute temperature of the system, respectively,  $U_{\text{test}}$  is the interaction energy of the inserted test particle with the system,  $P_{\text{cav}}$  is the probability of finding a suitable empty cavity, and the brackets  $\langle \dots \rangle$  denote ensemble averaging.  $P_{\text{cav}}$  is directly obtained in the calculation as the ratio of the number of gridpoint representing cavities to the total number of gridpoints in the cell. The calculation provides also the fraction of the accessible free volume for the probe of radius  $R_{\text{cav}}$  immediately. It should be noted that in the case of  $R_{\text{cav}} = 0$  the  $P_{\text{cav}}$  probability is unity, and the original version of the particle insertion method (87) is given back. When the diffusion constant profile of the solute  $D(Z)$  is also determined (40,85,86) (e.g., by the force correlation method, *see ref. 40*), the experimentally accessible permeability coefficient of the solute  $P$  can also be calculated (40,85,86) using the inhomogeneous solubility-diffusion model of Marrink and Berendsen (85), as

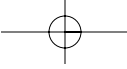
$$\frac{1}{P} = \int_{z_1}^z \frac{\exp[A(Z)/k_{\text{B}}T]}{D(Z)} dz. \quad (14)$$

#### Acknowledgments

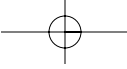
Pal Jedlovszky is supported by the Foundation for Hungarian Research and Higher Education as a Békésy György Fellow. P. J. acknowledges financial support of the Hungarian OTKA Foundation under Project no. T049673.

#### References

1. Jorgensen, W. L., Maxwell, D. S., and Tirado-Rives, J. (1996) Development and Testing of the OPLS All-Atom Force Field on Conformational Energetics and Properties of Organic Liquids. *J. Am. Chem. Soc.* **118**, 11,225–11,236.
2. Brooks, B. R., Bruckolieri, R. E., Olafson, B. D., States, D. J., Swaminathan, S., and Karplus, M. (1983) CHARMM: A program for macromolecular energy, minimization and dynamics calculation. *J. Comp. Chem.* **4**, 187–217, URL:<http://www.charmm.org>. April 1, 2007.
3. AMBER: Assisted model building with energy refinement, URL:<http://www.amber.ucsf.edu/amber/amber.htm>. April 1, 2007.
4. Gasteiger, J. and Marsali, M. (1980) Iterative partial equalization of orbital electronegativity—a rapid access to atomic charges. *Tetrahedron* **36**, 3219–3229.



5. GROMACS: The world's fastest molecular dynamics, URL:<http://www.gromacs.org/>. April 1, 2007.
6. Goetz, R. and Lipowsky, R. (1998) Computer simulation of bilayer membranes: Self-assembly and interfacial tension. *J. Chem. Phys.* **108**, 7397–7409.
7. Shelley, J. C., Shelley, M. Y., Reeder, R. C., Bandyopadhyay, S., and Klein, M. L. (2001) A Coarse Grain Model for Phospholipid Simulations. *J. Phys. Chem. B* **105**, 4464–4470.
8. Martí, J. (2004) A molecular dynamics transition path sampling study of model lipid bilayer membranes in aqueous environment. *J. Phys. Condens. Matter.* **16**, 5669–5678.
9. Marrink, S. J., de Vries, A. H., and Mark, A. E. (2004) Coarse Grained Model for Semiquantitative Lipid Simulations. *J. Phys. Chem. B* **108**, 750–760.
10. Jedlovszky, P. and Mezei, M. (1999) Grand canonical ensemble Monte Carlo simulation of a lipid bilayer using extension biased rotations. *J. Chem. Phys.* **111**, 10,770–10,773.
11. Dolan, E. A., Venable, R. M., Pastor, R. W., and Brooks, B. R. (2002) Simulations of membranes and other interfacial systems using P2<sub>1</sub> and P<sub>c</sub> periodic boundary conditions. *Biophys. J.* **82**, 2317–2325.
12. Gumbart, J., Wang, Y., Aksimentiev, A., Tajkhorshid, E., and Schulten, K. (2005) Molecular dynamics simulations of proteins in lipid bilayers. *Curr. Opin. Struct. Biol.* **15**, 423–431.
13. Neumann, M. (1985) The dielectric constant of water. Computer simulations with the MCY potential. *J. Chem. Phys.* **82**, 5663–5672.
14. Ewald, P. (1924) Die Berechnung optischer und elektrostatischer Gitterpotentiale. *Ann. Phys.* **64**, 253–287.
15. Campbell, E. S. (1963) Existence of a “well defined” specific energy for an ionic crystal; justification of Ewald’s formulae and their use to deduce equations for multipole lattices. *J. Phys. Chem. Solids.* **24**, 197–208.
16. Essman, U., Perera, L., Berkowitz, M. L., Darden, T., Lee, H., and Pedersen, L. G. (1995) A smooth particle mesh Ewald method. *J. Chem. Phys.* **103**, 8577–8593.
17. Yeh, I. C. and Berkowitz, M. L. (1999) Ewald summation for systems with slab geometry. *J. Chem. Phys.* **111**, 3155–3162.
18. Chiu, S. W., Clark, M., Balaji, V., Subramaniam, S., Scott, H. L., and Jakobsson, E. (1995) Incorporation of Surface Tension into Molecular Dynamics Simulation of an Interface. A Fluid Phase Lipid Bilayer Membrane. *Biophys. J.* **69**, 1230–1245.
19. Tieleman, D. P. and Berendsen, H. J. C. (1996) Molecular dynamics simulation of a fully hydrated dipalmitoylphosphatidylcholine bilayer with different macroscopic boundary conditions and parameters. *J. Chem. Phys.* **103**, 4871–4880.
20. Mezei, M. (1980) A cavity-biased ( $T, V, \mu$ ) Monte Carlo method for the computer simulation of fluids. *Mol. Phys.* **40**, 901–906.
21. Mezei, M. (1987) Grand-canonical ensemble Monte Carlo simulation of dense fluids: Lennard-Jones, soft spheres and water. *Mol. Phys.* **61**, 565–582. Erratum (1989) **67**, 1207–1208.
22. Mezei, M. (2002) On the potential of Monte Carlo methods for simulating macromolecular assemblies, in *Third International Workshop for Methods for Macromolecular Modeling Conference Proceedings*, (Gan, H. H. and Schlick, T., eds.), Springer, New York, pp. 177–196.
23. Chiu, S. W., Jakobsson, E., and Scott, H. L. (2001) Combined Monte Carlo and Molecular Dynamics Simulation of Hydrated Lipid-Cholesterol Lipid Bilayers at Low Cholesterol Concentration. *Biophys. J.* **80**, 1104–1114.
24. Chiu, S. W., Jakobsson, E., and Scott, H. L. (2001) Combined Monte Carlo and molecular dynamics simulation of hydrated dipalmitoyl-phosphatidylcholine–cholesterol lipid bilayers. *J. Chem. Phys.* **114**, 5435–5443.
25. Ebersole, B. J., Visiers, I., Weinstein, H., and Sealfon, S. C. (2003) Molecular basis of partial agonism: orientation of indoleamine ligands in the binding pocket of the human serotonin 5-HT2A receptor determines relative efficacy. *Mol. Pharm.* **63**, 36–43.



26. Allen, M. P. and Tildesley, D. J. (1986) *Computer simulation of liquids*. Clarendon Press, Oxford.
27. Ryckaert, J. P., Ciccotti, G., and Berendsen, H. J. C. (1977) Numerical integration of cartesian equation of motion of a system with constraints; molecular dynamics of n-alkanes. *J. Comp. Phys.* **23**, 327–341.
28. Metropolis, N. A., Rosenbluth, A. W., Rosenbluth, M. N., Teller, A. H., and Teller, E. (1953) Equation of state calculation by fast computing machines. *J. Chem. Phys.* **21**, 1087–1092.
29. Rosenbluth, M. N. and Rosenbluth, A. W. (1955) Monte Carlo calculation of the average extension of molecular chains. *J. Chem. Phys.* **23**, 356–359.
30. Siepmann, I. and Frenkel, D. (1992) Configurational bias Monte Carlo: a new sampling scheme for flexible chains. *Mol. Phys.* **75**, 59–70.
31. Dodd, L. R., Boone, T. D., and Theodorou, D. N. (1993) A concerted rotation algorithm for atomistic Monte Carlo simulation of polymer melts and glasses. *Mol. Phys.* **78**, 961–996.
32. Mezei, M. (2003) Efficient Monte Carlo sampling for long molecular chains using local moves, tested on a solvated lipid bilayer. *J. Chem. Phys.* **118**, 3874–3879.
33. Noguti, T. and Go, N. (1985) Efficient Monte Carlo method for simulation of fluctuating conformations of native proteins. *Biopolymers* **24**, 527–546.
34. Marrink, S. J., Tieleman, D. P., and Mark, A. E. (2000) Molecular Dynamics Simulations of the Kinetics of Spontaneous Micelle Formation. *J. Phys. Chem. B* **104**, 12,165–12,173.
35. URL:<http://thallium.bsd.uchicago.edu/Roux Lab/>; April 1, 2007.
36. De Loof, H. D., Harvey, S. C., Segrest, J. P., and Pastor, R. W. (1991) Mean field stochastic boundary molecular dynamics simulation of a phospholipid in a membrane. *Biochemistry* **30**, 2099–2113.
37. Pastor, R. W., Venable, R. M., and Karplus, M. (1991) Model for the structure of the lipid bilayer. *Proc. Natl. Acad. Sci. USA* **88**, 892–896.
38. Smondyrev, A. M. and Berkowitz, M. L. (1999) Structure of Dipalmitoylphosphatidylcholine/Cholesterol Bilayer at Low and High Cholesterol Concentrations: Molecular Dynamics Simulation. *Biophys. J.* **77**, 2075–2089.
39. Jedlovszky, P. and Mezei, M. (2003) Effect of Cholesterol on the Properties of Phospholipid Membranes. 1. Structural Features. *J. Phys. Chem. B* **107**, 5311–5321.
40. Marrink, S. J. and Berendsen, H. J. C. (1994) Simulation of Water Transport through a Lipid Membrane. *J. Phys. Chem.* **98**, 4155–4168.
41. Rabinovich, A. L., Balabaev, N. K., Alinchenko, M. G., Voloshin, V. P., Medvedev, N. N., and Jedlovszky, P. (2005) Computer simulation study of intermolecular voids in unsaturated phosphatidylcholine lipid bilayers. *J. Chem. Phys.* **122**, 084906. 12 pages.
42. Hyvönen, M. T., Rantala, T. T., and Ala-Korpela, M. (1997) Structure and Dynamic Properties of Diunsaturated 1-Palmitoyl-2-Linoleoyl-*sn*-Glycero-3-Phosphatidylcholine Lipid Bilayer from Molecular Dynamics Simulation. *Biophys. J.* **73**, 2907–2923.
43. Heller, H., Schaefer, M., and Schulten, K. (1993) Molecular Dynamics Simulation of a Bilayer of 200 Lipids in the Gel and Liquid-Crystal Phases. *J. Phys. Chem.* **97**, 8343–8360.
44. Tu, K., Tobias, D. J., and Klein, M. L. (1995) Constant Pressure and Temperature Molecular Dynamics Simulation of a Fully Hydrated Liquid Crystal Phase Dipalmitoylphosphatidylcholine Bilayer. *Biophys. J.* **69**, 2558–2562.
45. Tu, K., Klein, M. L., and Tobias, D. J. (1998) Constant-Pressure Molecular Dynamics Investigation of Cholesterol Effects in a Dipalmitoylphosphatidylcholine Bilayer. *Biophys. J.* **75**, 2147–2156.
46. Zubrzycki, I. Z., Xu, Y., Madrid, M., and Tang, P. (2000) Molecular dynamics simulation of a fully hydrated dimyristoylphosphatidylcholine membrane in liquid-crystalline phase. *J. Chem. Phys.* **112**, 3437–3441.
47. Saiz, L. and Klein, M. L. (2001) Structural Properties of a Highly Polyunsaturated Lipid Bilayer from Molecular Dynamics Simulations. *Biophys. J.* **81**, 204–216.

48. Husslein, T., Newns, D. M., Pattnaik, P. C., Zhong, Q., Moore, P. B., and Klein, M. L. (1998) Constant pressure and temperature molecular-dynamics simulation of the hydrated diphyl-phosphatidylcholine lipid bilayer. *J. Chem. Phys.* **109**, 2826–2832.

49. Pasenkiewicz-Gierula, M., Takaoka, Y., Miyagawa, H., Kitamura, K., and Kusumi, A. (1999) Charge Pairing of Headgroups in Phosphatidylcholine Membranes: A Molecular Dynamics Simulation Study. *Biophys. J.* **76**, 1228–1240.

50. Saiz, L. and Klein, M. L. (2002) Electrostatic interactions in neutral model phospholipid bilayer by molecular dynamics simulations. *J. Chem. Phys.* **116**, 3052–3057.

51. Åman, K., Lindahl, E., Edholm, O., Håkansson, P., and Westlund, P. O. (2003) Structure and Dynamics of Interfacial Water in an  $L_\alpha$  Phase Lipid Bilayer from Molecular Dynamics Simulations. *Biophys. J.* **84**, 102–115.

52. Rabinovich, A. L., Ripatti, P. O., Balabaev, N. K., and Leermakers, F. A. M. (2003) Molecular dynamics simulations of hydrated unsaturated lipid bilayers in the liquid-crystal phase and comparison to self-consistent field modelling. *Phys. Rev. E* **67**, 011909. 14 pages.

53. Snyder, R. G., Tu, K., Klein, M. L., Mendelsohn, R., Strauss, H. L., and Sun, W. (2002) Acyl Chain Conformation and Packing in Dipalmitoylphosphatidylcholine Bilayers from MD Simulation and IR Spectroscopy. *J. Phys. Chem. B* **106**, 6273–6288.

54. Hofssäß, C., Lindahl, E., and Edholm, O. (2003) Molecular Dynamics Simulations of Phospholipid Bilayers with Cholesterol. *Biophys. J.* **84**, 2192–2206.

55. Shinoda, W., Mikami, M., Baba, T., and Hato M. (2003) Molecular Dynamics Study on the Effect of Chain Branching on the Physical Properties of Lipid Bilayers: Structural Stability. *J. Phys. Chem. B* **107**, 14,030–14,035.

56. López-Cascales, J. J., García de la Torre, J., Marrink, S. J., and Berendsen, H. J. C. (1996) Molecular dynamics simulations of a charged biological membrane. *J. Chem. Phys.* **104**, 2713–2720.

57. van der Ploeg, P. and Berendsen, H. J. C. (1982) Molecular dynamics simulation of a bilayer membrane. *J. Chem. Phys.* **76**, 3271–3276.

58. Jedlovszky, P. and Mezei, M. (2001) Orientational Order of the Water Molecules Across a Fully Hydrated DMPC Bilayer. A Monte Carlo Simulation Study. *J. Phys. Chem. B* **105**, 3614–3623.

59. Pandit, S. A., Bostick, D., and Berkowitz, M. L. (2003) An algorithm to describe molecular scale rugged surfaces and its application to the study of a water/lipid bilayer interface. *J. Chem. Phys.* **119**, 2199–2205.

60. Gawrisch, K., Ruston, D., Zimmemberg, J., Parsegian, V. A., Rand, R. P., and Fuller, N. (1992) Membrane dipole potentials, hydration forces, and the ordering of water at membrane surfaces. *Biophys. J.* **61**, 1213–1223.

61. Pasenkiewicz-Gierula, M., Takaoka, Y., Miyagawa, H., Kitamura, K., and Kusumi, A. (1997) Hydrogen Bonding of Water to Phosphatidylcholine in the Membrane As Studied by a Molecular Dynamics Simulation: Location, Geometry, and Lipid-Lipid Bridging via Hydrogen-Bonded Water. *J. Phys. Chem. A* **101**, 3677–3691.

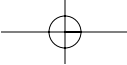
62. Pasenkiewicz-Gierula, M., Rög, T., Kitamura, K., and Kusumi, A. (2000) Cholesterol Effects on the Phosphatidylcholine Bilayer Polar Region: A Molecular Simulation Study. *Biophys. J.* **78**, 1517–1521.

63. Chiu, S. W., Jakobsson, E., Mashl, R. J., and Scott, H. L. (2002) Cholesterol-Induced Modifications in Lipid Bilayers: A Simulation Study. *Biophys. J.* **83**, 1842–1853.

64. Shinoda, K., Shinoda, W., Baba, T., and Mikami, M. (2004) Comparative molecular dynamics study of ether- and ester-linked phospholipid bilayers. *J. Chem. Phys.* **121**, 9648–9654.

65. Jedlovszky, P., Medvedev, N. N., and Mezei, M. (2004) Effect of Cholesterol on the Properties of Phospholipid Membranes. 3. Local Lateral Structure. *J. Phys. Chem. B* **108**, 465–472.

66. Jedlovszky, P., Pártay, L., and Mezei, M. (2007) The structure of the zwitterionic headgroups in a DMPC bilayer as seen from Monte Carlo simulation: Comparisons with ionic solutions. *J. Mol. Liquids*, **131–132**, 225–234.



67. Shinoda, W. and Okazaki, S. (1998) A Voronoi analysis of lipid area fluctuation in a bilayer. *J. Chem. Phys.* **109**, 2199–2205.
68. Falck, E., Patra, M., Karttunen, M., Hyvönen, M. T., and Vattulainen, I. (2004) Lessons of Slicing Membranes: Interplay of Packing, Free Area, and Lateral Diffusion in Phospholipid/Cholesterol Bilayers. *Biophys. J.* **87**, 1076–1091.
69. Jedlovszky, P., Vincze, Á., and Horvai, G. (2002) New insight into the orientational order of water molecules at the water/1,2-dichloroethane interface: a Monte Carlo simulation study. *J. Chem. Phys.* **117**, 2271–2280.
70. Jedlovszky, P., Vincze, Á., and Horvai, G. (2004) Full description of the orientational statistics of molecules near interfaces. Water at the interface with  $\text{CCl}_4$ . *Phys. Chem. Chem. Phys.* **6**, 1874–1879.
71. Cantor, R. S. (1999) Lipid Composition and the Lateral Pressure Profile in Bilayers. *Biophys. J.* **76**, 2625–2639.
72. Marrink, S. J., Sok, R. M., and Berendsen, H. J. C. (1996) Free volume properties of a simulated lipid membrane. *J. Chem. Phys.* **104**, 9090–9099.
73. Okabe, A., Boots, B., Sugihara, K., and Chiu, S. N. (2000) *Spatial Tessellations: Concepts and Applications of Voronoi Diagrams*. John Wiley, Chichester.
74. Jedlovszky, P. and Mezei, M. (2000) Calculation of the Free Energy Profile of  $\text{H}_2\text{O}$ ,  $\text{O}_2$ ,  $\text{CO}$ ,  $\text{CO}_2$ ,  $\text{NO}$ , and  $\text{CHCl}_3$  in a Lipid Bilayer with a Cavity Insertion Variant of the Widom Method. *J. Am. Chem. Soc.* **122**, 5125–5131.
75. Jedlovszky, P. and Mezei, M. (2003) Effect of Cholesterol on the Properties of Phospholipid Membranes. 2. Free Energy Profile of Small Molecules. *J. Phys. Chem. B* **107**, 5322–5332.
76. Falck, E., Patra, M., Karttunen, M., Hyvönen, M. T., and Vattulainen, I. (2004) Impact of cholesterol on voids in phospholipid membranes. *J. Chem. Phys.* **121**, 12,676–12,689.
77. Alinchenko, M. G., Anikeenko, A. V., Medvedev, N. N., Voloshin, V. P., Mezei, M., and Jedlovszky, P. (2004) Morphology of Voids in Molecular Systems. A Voronoi-Delaunay Analysis of a Simulated DMPC Membrane. *J. Phys. Chem. B* **108**, 19,056–19,067.
78. Alinchenko, M. G., Voloshin, V. P., Medvedev, N. N., Mezei, M., Pártay, L., and Jedlovszky, P. (2005) Effect of Cholesterol on the Properties of Phospholipid Membranes. 4. Interatomic Voids. *J. Phys. Chem. B* **109**, 16,490–16,502.
79. Bassolino-Klimas, D., Alper, H. E., and Stouch, T. R. (1995) Mechanism of Solute Diffusion through Lipid Bilayer Membranes by Molecular Dynamics Simulation. *J. Am. Chem. Soc.* **117**, 4118–4129.
80. López-Cascales, J. J., Hernández Cifre, J. G., and García de la Torre, J. (1998) Anaesthetic Mechanism on a Model Biological Membrane: A Molecular Dynamics Simulations Study. *J. Phys. Chem. B* **102**, 625–631.
81. Söderhäll, J. A. and Laaksonen, A. (2001) Molecular Dynamics Simulation of Ubiquinone inside a Lipid Bilayer. *J. Phys. Chem. B* **105**, 9308–9315.
82. Duong, T. H., Mehler, E. L., and Weinstein, H. (1999) Molecular Dynamics Simulation of Membranes and a Transmembrane Helix. *J. Comp. Phys.* **151**, 358–387.
83. Bandyopadhyay, S., Tarek, M., and Klein, M. L. (1999) Molecular Dynamics Study of a Lipid–DNA Complex. *J. Phys. Chem. B* **103**, 10,075–10,080.
84. Pandit, S. A., Vasudevan, S., Chiu, S. W., Mashl, R. J., Jakobsson, E., and Scott, H. L. (2004) Sphingomyelin-Cholesterol Domains in Phospholipid Membranes: Atomistic Simulation. *Biophys. J.* **87**, 1092–1100.
85. Marrink, S. J. and Berendsen, H. J. C. (1996) Permeation Process of Small Molecules across Lipid Membranes Studied by Molecular Dynamics Simulations. *J. Phys. Chem.* **100**, 16,729–16,738.
86. Shinoda, W., Mikami, M., Baba, T., and Hato, M. (2004) Molecular Dynamics Study on the Effect of Chain Branching on the Physical Properties of Lipid Bilayers: 2. Permeability. *J. Phys. Chem. B* **108**, 9346–9356.
87. Widom, B. (1963) Some Topics in the Theory of Fluids. *J. Chem. Phys.* **39**, 2808–2812.